EUROPEAN ORGANIZATION FOR NUCLEAR RESEARCH

CERN/EP 79-41
27 April 1979

DALITZ ARRAYS OF THE ω, ϕ, A_2 AND A_1 RESONANCES

F. del Aguila(*), M. Aguilar-Benitez(**), M. Cerrada(***), M.G. Doncel(*)
and Ph. Gavillet

CERN, Geneva, Switzerland

ABSTRACT

After summarizing the properties of the so-called Dalitz Array (DA), which is a genuine characteristics of a resonance, we determine those of the well known ω, ϕ and A_2 resonances produced in the $K^-p \to \pi^+\pi^-\pi^0\Lambda$ final state at 4.2 GeV/c. A tentative measurement of the DA of the A_1 meson produced backwards in the reaction $K^-p \to \pi^+\pi^+\pi^-\Sigma^-$ is also presented. The data for this analysis come from the high statistics (130 events/μb) experiment performed by the ACNO Collaboration.

Submitted to Nuclear Physics B

(*) On leave of absence from Universidad Autonoma de Barcelona, Bellaterra, Barcelona, Spain.

(**) On leave of absence from Junta de Energia Nuclear, Madrid, Spain.

(***) Max-Planck Institut, Munich, Germany.

FDA/jl

1. INTRODUCTION

A large amount of work has been devoted in the past to extract properties of three-body resonances from the analysis of the decay Dalitz Plot (DP). The study of such distributions and the use of some simplifying assumptions permitted to determine for instance the spin parity assignment of the ω resonance [1,2]. Among the various generalizations of the method, that of Zemach [3] has been widely used in spin parity measurements and partial wave analyses. In this work, we follow a different approach based on a "democratic" treatment of three-particle systems [4-7].

In order to describe the decay DP distribution we introduce a complete set of orthonormal functions on the DP. The average values of these functions (experimental moments) form an array of numbers which will be called Dalitz Array (DA). Geometrically speaking, these functions supply a convenient orthonormal basis for the real Hilbert space of DP distributions. The experimental DP distribution can then be considered as a vector in this space and its coordinates with respect to this basis are the DA. Any given resonance decaying into three particles is characterised by its DA, which has to be considered as another intrinsic property of the state. Therefore, the measurement of the DA of a resonance (produced cleanly in a given reaction) can be very useful when trying to disentangle the contribution of such a resonance in a rather complicated final state. The DA affords a method to detect the presence of the resonance and to measure its production cross section. On the other hand, any dynamical model gives a theoretical DA, which correponds to a well defined point in the metrical space of DP distributions. The distance between this theoretical point and the experimental point is independent of the orthonormal basis taken in this Hilbert space and provides a test of the theoretical model under investigation.

In principle, the DA consists of an infinite number of elements. However, theoretical and phenomenological considerations [4] suggest that only the first few terms, corresponding to small values of the so called "togetherness" (sect. 2) will be significant.

An advantage of the approach presented here is that the constraints imposed by Bose statistics can be formulated in a rather simple form [5-7]. When the three mesons belong to the same isospin multiplet, these constraints are particularly strong. Such is the case of the ω, φ, A_2 and A_1 resonances decaying into three pions. The measurement of the DA of these four resonances will be discussed in this paper.

The paper is organized as follows. In sect. 2, we outline the formalism and the method of analysis. The basic functions and formulae are explicitly given for the cases considered in this work. Some relevant features of the data, as well as the DA determination for the ω, φ and A_2, are presented in sect. 3. The study of the $A_1^+ \to \pi^+\pi^+\pi^-$ decay is discussed in sect. 4. A summary of the work and some final remarks are given in sect. 5.

2. THE BASIC FORMALISM

The DP variables ρ and φ to be used in this analysis [6] are defined in table 1(a). The mass difference between the charged and neutral pions has been neglected. The polar variable ρ is zero at the centre of the DP and is normalized to one at its boundary. The azimuthal variable φ is such that the element of surface ρdρdφ is preserved when changing the DP variables. To describe the experimental distribution in the DP, we use the functions $G^{\lambda\mu}(\rho, \phi)$ which are discussed elsewhere [7]. They satisfy the orthonormality conditions

$$\frac{1}{\pi}\int_0^1\int_0^{2\pi} G^{\lambda\mu}(\rho, \phi)^* \; G^{\lambda'\mu'}(\rho, \phi)\rho d\rho d\phi = \delta_{\lambda\lambda'}\,\delta_{\mu\mu'} \qquad (1)$$

where λ, μ are indices of the SU(3) group. The index λ has to be even and positive, and μ can have the values λ, λ-4, ..., -λ. The complex functions $G^{\lambda\mu}(\rho, \phi)$ satisfy the relation

$$G^{\lambda-\mu}(\rho, \phi) = G^{\lambda\mu}(\rho, \phi)^*. \qquad (2)$$

The explicit expressions of $G^{\lambda\mu}(\rho, \phi)$ for the specific cases considered here are given in table 1(b).

The DP distribution can be expressed as

$$I(\rho,\ \phi) = \sum_{\lambda\mu} (q^{\lambda\mu})^* \ G^{\lambda\mu}(\rho,\ \phi). \tag{3}$$

Using eq. (1) the DA moments are written as

$$q^{\lambda\mu} = \frac{1}{\pi} \int_0^1 \int_0^{2\pi} I(\rho,\ \phi)\ G^{\lambda\mu}(\rho,\phi)\rho d\rho d\phi \tag{4a}$$

and for an experimental sample of N events they can be approximated by

$$q^{\lambda\mu} = \frac{1}{N} \sum_{i=1}^{N} G^{\lambda\mu}\ (\rho_i,\ \phi_i), \tag{4b}$$

where ρ_i, ϕ_i are the DP coordinates of the i-th event of the sample. Since $q^{\lambda\mu}$ is a complex number, for $\mu \neq 0$, we will use its real and imaginary parts properly normalized

$$q_R^{\lambda\mu} = (q^{\lambda\mu} + q^{\lambda-\mu})/\sqrt{2} = \sqrt{2}\ \mathrm{Re}\ q^{\lambda\mu}\ , \tag{5a}$$

$$q_I^{\lambda\mu} = (q^{\lambda\mu} - q^{\lambda-\mu})/\sqrt{2}\ i = \sqrt{2}\ \mathrm{Im}\ q^{\lambda\mu}\ . \tag{5b}$$

Basically, the moments $q^{\lambda\mu}$ fix the shape of the DP distribution. They are quadratic functions of the physical amplitudes describing the three-body decay. As discussed elsewhere [7], for a resonance decaying strongly into three spinless particles, these amplitudes can be labelled $a^{\lambda\mu(\delta\iota)}$. Here, the index λ can have even and odd values, according to the parity of the resonance and μ can take the values λ, $\lambda-2$, $\lambda-4, \ldots$, $-\lambda$. Eventually, two diacritical indices are needed: δ for distinguishing equal spin multiplets in the SO(3) reduction of a SU(3) representation, and ι for distinguishing equal isospin multiplets in the decomposition of the product of the three isomultiplets. The index λ is called togetherness and, from a classical point of view [4], gives a measurement of the proximity among the three particles when the three-body system is produced. From theoretical and phenomenological reasons we assume that in the decay of a resonance only the amplitudes with small values of λ are relevant. Thus, in table 2 (a) we present the first allowed amplitudes in the three-pion decay of resonances with quantum numbers $I(J^P) = 0(1^-)$, such as the ω and ϕ. The quadratic expressions of the allowed moments in terms of these amplitudes are also given. In table 2(b) and 2(c)-(d) similar quantities are given for the $A_2(I(J^P) = 1(2^+))$ and $A_1(I(J^P) = 1(1^+))$ resonances.

The moments defined in eq. (4) satisfy the normalization condition $q^{00} = 1$. In order to detect a resonance behaviour in a DP distribution and to determine the corresponding DA, it is convenient to measure the DP distribution as a function of the three-body invariant mass M. For this purpose, we introduce the unnormalized experimental moments

$$Q^{\lambda\mu} = \sum_i G^{\lambda\mu}(\rho_i, \phi_i) w_i , \tag{6a}$$

where the sum extends over all events in a given mass interval, and w_i is the experimental weight of the i-th event. The associated errors are given by

$$\Delta Q^{\lambda\mu} = \left\{ \sum_i (G^{\lambda\mu}(\rho_i, \phi_i)\, w_i)^2 \right\}^{\frac{1}{2}} \tag{6b}$$

In the ideal situation of a resonance produced with no background, only certain $Q^{\lambda\mu}$ moments are expected to have non zero values. A measurement of the DA ($q^{\lambda\mu}$ values) will be obtained by fitting the $Q^{\lambda\mu}$ moments with the following expression

$$Q^{\lambda\mu}(M) = q^{\lambda\mu} R(M), \tag{7a}$$

where the function R(M) is assumed to have a Breit-Wigner form

$$R(M) = I_R M_R^2 \Gamma_R^2 \Big/ \left[(M^2 - M_R^2)^2 + M_R^2 \Gamma_R^2 \right] \tag{7b}$$

with I_R being the intensity at $M = M_R$, and M_R, Γ_R the mass and the width of the resonance.

Unfortunately, a certain amount of background is always present and contributes to the different $Q^{\lambda\mu}$. This background comes either from the reflection of other competitive channels or from other partial waves of the three-body system under consideration. This contamination is taken into account by including an additional term in 7(a)

$$Q^{\lambda\mu}(M) = q^{\lambda\mu}R(M) + B^{\lambda\mu}(M). \qquad (7c)$$

The background term $B^{\lambda\mu}(M)$ is parametrized in terms of smooth functions of M. The validity of expression (7c) rests on the following two assumptions:

(a) Reflections from other channels are not strong enough to produce significant structures in $Q^{\lambda\mu}$.

(b) There is no significant non resonant contribution with the same quantum numbers of the resonance (otherwise interference terms should appear in (7c)).

As it will be discussed in sect. 3 these two hypothesis are approximately satisfied in the cases under study.

It is important to notice that the elements $q^{\lambda\mu}$ of the DA are not independent. Since they are quadratic functions of the significant decay amplitudes (given explicitly in table 2 for the cases of interest) they are constrained by the positivity and rank conditions. From this, it follows that the best approach to determine the DA is to use, as basic parameters in the fit, the decay amplitudes and construct from them the normalized theoretical moments which will automatically satisfy all these conditions.

The number of resonance events for a given reaction is usually measured from the distribution of the Q^{00} moment defined in eq.(6). An alternative procedure is to use as estimator the distribution

$$Q = \sum_{\lambda\mu} q^{\lambda\mu} Q^{\lambda\mu} \Big/ \sum_{\lambda\mu} \left| q^{\lambda\mu} \right|^2 , \qquad (8)$$

where $q^{\lambda\mu}$ is the DA of the resonance measured in a precise previous experiment and $Q^{\lambda\mu}$ are unnormalized moments defined in eq. (6). When the background can be neglected, both techniques give the same number of events since the vector $Q^{\lambda\mu}$ is Q^{00} times the vector $q^{\lambda\mu}$. On the other hand, it is possible to extend the sum in eq (8) to any part of the DA (for instance, to all terms except the first one, with $\lambda = \mu = 0$). Then, assuming that eq. (8) contains many significant terms, the background contribution will be strongly suppressed, since it consists of an arbitrary vector contained in $Q^{\lambda\mu}$, and only its projection on $q^{\lambda\mu}$ contributes to eq. (8). Notice that according to the definition given in eq. (6a), Q is the experimental moment

$$Q = \sum_i G(\rho_i, \phi_i)\, w_i \tag{9a}$$

of the function

$$G(\rho, \phi) = \sum_{\lambda\mu} q^{\lambda\mu} G^{\lambda\mu}(\rho, \phi) \Big/ \sum_{\lambda\mu} \left|q^{\lambda\mu}\right|^2 , \tag{9b}$$

which we call Dalitz series and which is specified by the DA of the resonance ($q^{\lambda\mu}$).

3. DALITZ ARRAYS OF THE ω, ϕ AND A_2

The data for this analysis come from an exposure of the CERN 2m bubble chamber to a K^- beam of average momentum 4.15 GeV/c. The experiment has been made by an Amsterdam-CERN-Nijmegen-Oxford Collaboration and the statistical sensitivity of the sample is $\sim$ 130 events/μbarn. In the final state $K^- p \to \pi^+\pi^-\pi^0\Lambda$, the 3π system produced in the forward direction has been previously studied with a method of partial wave decomposition [8]. A more complete description of the experimental details of the data sample can be found elsewhere [8,9]. The sample to be used in this study is made of 60 949 unweighted events. In fig. 1 the $\pi^+\pi^-\pi^0$ effective mass distribution is presented. The ω resonance is copiously produced, both in the forward and backward hemispheres. A clear enhancement around $M(\pi^+\pi^-\pi^0) \sim 1.0$ GeV is also present, but it is mainly restricted to the most peripheral momentum transfer region. This effect is a superposition of the ϕ meson and the $\eta' \to \pi^+\pi^-\gamma$ decay (where the γ has been wrongly interpreted as a π^0). The A_2 resonance is hardly visible in the mass distribution. However, the results from the Partial Wave Analysis [8] give a significant cross section (15.7 ± 1.5 μb) in the region $|t| < 1.0$ GeV^2.

In order to extract the DA of the ω, ϕ and A_2 we have performed χ^2 fits to the unnormalized $Q^{\lambda\mu}(M)$ moments defined in eq. (6). The theoretical form of the moments is given in eq. (7c) and assumes no interference effects with the underlying background. We have checked that the important production of $\Sigma(1385)$ states gives small and structureless contribution to the moments of the 3π Dalitz plot in the regions under investigation. On the other hand, the partial wave analysis shows that no background waves with the same spin are significantly present below the ω, ϕ and A_2 resonances. These considerations justify the use of eq. (7c).

The background term $B^{00}(M)$ was parametrized as a low order polynomial in the 3π mass. The other $B^{\lambda\mu}(M)$ terms were described as products of the $B^{00}(M)$ times first order polynomials. This very flexible parametrization appears to be more appropriate for small mass regions and for this reason it was decided to fit the three resonances separately.

The number of parameters in the fit depends on the number of moments to be used and on the number of basic decay amplitudes. In the cases to be considered we are dealing with 25 parameters: one giving the intensity of the resonance contribution, four describing the three normalized decay amplitudes and twenty for the polynomial backgrounds (two per fitted moment). In this study resolution effects were not included and the width of the resonance was taken as the observed width. Although the resonance parameters were initially fixed, they were fitted in a subsequent step of the analysis.

3.1 Dalitz Array of the ω

The mass region of the 3π system considered for the analysis of the ω was 0.73 - 0.83 GeV, divided in 20 bins of 5 MeV. It contains 5367 unweighted events. The background level is approximately 6%. Assuming three significant decay amplitudes (table 2(a)) there are ten non vanishing moments:

$$Q^{0,0},\ Q^{4,0},\ Q^{8,0},\ Q^{12,0},\ Q^{16,0},\ Q^{6,6},\ Q^{10,6},\ Q^{14,6},\ Q^{12,12},\ Q^{16,12}.$$

The experimental moments are displayed in fig.2. The solid lines represent the results of the fit using expression (7c) and the dashed lines the background contribution ($B^{\lambda\mu}(M)$). The fit reproduces adequately the data. The ω production cross section measured is in perfect agreement with the results obtained in ref. [9]. The normalized amplitudes and the DA obtained from the fit are given in table 3(a).

3.2 Dalitz Array of the ϕ

The mass region used for the analysis of the ϕ was 1.005- 1.045 GeV divided in 8 bins of 5 MeV. The contamination from the η' can be considered negligible above 1.0 GeV. In order to enrich the ϕ content of the sample, the peripheral selection $0.65 < \cos\theta_{p,\Lambda} < 1.00$ was imposed. The final sample contains 900 unweighted events and the experimental moments used were the same ones listed in the case of the ω. In spite of the large background ($\sim$ 50%) a reasonable fit was obtained, as can be seen in fig. 3. The resonance contribution is found to be in good agreement with that obtained in the Partial Wave Analysis of ref. [8]. The amplitudes and the DA are presented in table 3(b).

It is interesting to remark that the ω and ϕ resonances have different DA, although the two resonances have the same spin-parity. For the ω, the first three amplitudes satisfy the inequality $|a^{2,0}| >> |a^{6,0}| >> |a^{8,6}|$. However, since the amplitude $a^{8,6}$ is in phase with $a^{2,0}$ a small asymmetry appears in the azimuthal DP distribution. For the ϕ, the $a^{8,6}$ amplitude and the associated asymmetry are relatively more important. These observations might be related to the presence of ρ bands inside the DP.

3.3 Dalitz Array of the A_2

The mass region considered for the study of the A_2 was 1.1 - 1.5 GeV, divided in 10 bins of 40 MeV. After imposing the peripheral selection $0.65 < \cos\theta_{p,\Lambda} < 1.00$ the data sample contains 8930 unweighted events. In a preliminary analysis only the first three amplitudes $a^{3,1}$, $a^{5,1}$, $a^{5,3}$ were considered. They give rise to the moments

$$Q^{0,0},\ Q^{4,0},\ Q^{8,0},\ Q^{2,2},\ Q^{6,2},\ Q^{10,2},\ Q^{4,4},\ Q^{8,4},\ Q^{6,6},\ Q^{10,6}.$$

The fits lead to a negligible value of the amplitude $a^{5,3}$ and to an underestimation of the experimental moment $Q^{8,0}$. These results and the observation that the moment $Q^{12,0}$ shows some structure in this mass region suggesting to replace the amplitude $a^{5,3}$ by the $a^{7,1}$. The new moments considered in the analysis were now

$Q^{0,0}$, $Q^{4,0}$, $Q^{8,0}$, $Q^{12,0}$, $Q^{2,2}$, $Q^{6,2}$, $Q^{10,2}$, $Q^{14,2}$.

The study of the A_2 is rather difficult due to the large amount of background and the large mass interval that has to be considered. We have checked the stability of the results by performing various fits using different data samples (more restrictive cuts on the production variable $\cos\theta_{p,\Lambda}$, antiselection of the important $\Sigma^+(1385)$ and $\Sigma^0(1385)$ contributions) and different background parametrizations. Basically, we get compatible Dalitz arrays in all the fits. The best fit was obtained when the $\Sigma^+(1385)$ and $\Sigma^0(1385)$ states were removed with the cuts $1.34 < M(\Lambda\pi) < 1.44$ GeV, the selection $0.75 < \cos\theta_{p,\Lambda} < 1.00$ was imposed (4076 unweighted events remain) and the background term $B^{00}(M)$ was parametrized as the product of a parabola, vanishing at the two limits of the phase space, times a linear form in the mass. The DA obtained in this fit is shown in table 3(c). The experimental moments $Q^{\lambda\mu}$ and the fitted values are presented in fig. 4.

As indicated in sect. 2, the knowledge of the DA permits to measure the resonance contribution in a given final state by using the experimental moment of the Dalitz series (eq. (9)). Since the A_2 is produced with a large background, it is interesting to test the method here. As seen in figs 5(a,c) the A_2 is barely visible in the forward hemisphere and shows no signal in the backward hemisphere at the level of the 3π mass distributions (Q^{00}). However, the experimental moment of the Dalitz series (defined by the DA previously obtained) shows significant resonance like signals in the A_2 region (figs 5(b,d)). By fitting these distributions with an incoherent superposition of a Breit-Wigner form and a smooth background term, we have obtained the following values for the forward and backward cross sections

$$\sigma_F(K^-p \to A_2\Lambda) = 19.4 \pm 4.0 \ \mu b,$$

$$\sigma_B(K^-p \to A_2\Lambda) = 13.5 \pm 3.5 \ \mu b.$$

In the previous study of the 3π system [8] with a technique of Partial Wave Analysis, the cross section for A_2 production was calculated to be $\sigma = 15.7 \pm 1.5$ μb in the momentum transfer region $|t| < 1.0$ GeV^2. Using the value of the moment of the Dalitz series, the value $\sigma = 14 \pm 2.5$ μb was obtained in very good agreement with the previous determination.

It is important to notice that the amplitudes and DA of the A_2 have being obtained for the $\pi^+\pi^-\pi^0$ decay mode. The amplitudes are isospin invariant, but the coefficients in table 2(b) giving the DA in terms of the amplitudes depend of the particle charges. However, in the case of the $A_2^+ \to \pi^+\pi^+\pi^-$ decay and for the amplitudes $a^{3,1}$, $a^{5,1}$, $a^{7,1}$, these coefficients are the same. Thus, amplitudes and DA are in this case identical to those obtained for the $A_2^0 \to \pi^+\pi^-\pi^0$ decay. This DA will be used below in the study of the A_1^+ region.

4. DALITZ ARRAY OF THE A_1

For the study of the DA of the A_1, the reaction

$$K^-p \to \pi^+\pi^+\pi^-\Sigma^-$$

will be considered. This final state has been previously studied by the Amsterdam-CERN-Nijmegen-Oxford Collaboration in a search for backward production of meson resonances [10]. The data sample is made of 13 151 unweighted events. The effective mass distribution of the three-pion system produced in the backward region ($\cos\theta_{p,\Sigma^-} < -0.75$) is shown in fig. 6. Two enhancements are clearly seen in the mass spectrum. One corresponds to the A_2 resonance and the other signal is centred around 1.1 GeV, where the diffractive A_1 effect has been observed. These bumps cannot be explained by the reflections of known hyperon resonances and are enhanced when the $\pi^+\pi^-$ system is constrained to be in the ρ mass region ($0.62 < M(\pi^+\pi^-) < 0.88$ GeV). An analysis of the $\pi^+\pi^+\pi^-$ decay DP using the Zemach formalism has shown that these effects are associated to the waves $2^+(\rho\pi)$ and $1^+S(\rho\pi)$ respectively. The parameters of the A_1 effect obtained in ref. [10] are

$$M = 1.041 \pm 0.013 \text{ GeV} \qquad \Gamma = 0.230 \pm 0.050 \text{ GeV}$$

and the total backward production cross section for $\Sigma^-A_1^+(1040)$, $A_1^+ \to \pi^+\pi^+\pi^-$ is (3.6 ± 0.5) μb, which after correcting for unseen A_1^+ decay modes becomes $\sigma = (7.2 \pm 1.0)$ μb.

In order to determine the DA of the A_1^+ we have selected events with the 3π effective mass in the region 0.41 – 1.45 GeV and in the backward production interval $-1.0 < \cos\theta_{p,\Sigma^-} < -0.75$. This mass region includes some A_2^+ production which has to be taken into account in order to fix the amount of background. The data sample contains 1411 unweighted events and was divided in 13 mass bins of 80 MeV. Six non-vanishing A_1^+ moments are expected

$$Q^{0,0},\ Q^{4,0},\ Q^{2,2},\ Q^{6,2},\ Q^{4,4},\ Q^{6,6},$$

when only three decay amplitudes are considered (table 2(c)). The experimental moments are shown in fig. 7. With the exception of $Q^{2,2}$ which shows a clear structure in the A_1^+ region, all the moments are small and compatible with zero within the large experimental errors.

The moments were fitted with expression (7c), where now the background term has the form

$$B^{\lambda\mu}(M) = (q')^{\lambda\mu}\, R'(M) + C^{\lambda\mu}(M), \tag{10}$$

$(q')^{\lambda\mu}$ and $R'(M)$ being the DA and Breit-Wigner form of the A_2^+ state. The number of parameters to be fitted in this case is 20: four for the three normalized amplitudes of the A_1^+, two for its mass and width, two for the intensities of the A_1^+ and A_2^+, and twelve for the background terms. DA and decay amplitudes for the A_1^+ are presented in table 3(d). We also give in table 3(e) the DA for the $A_1^0 \to \pi^+\pi^-\pi^0$ decay, obtained using the coefficients in table 2(d). The measured A_1 cross section is compatible with that found in ref. [10].

We complete this section with a final remark concerning A_2^+ production in this reaction and which has to be considered as a further check of the validity of the method. In the backward hemisphere, the A_2^+ cross section obtained using the Dalitz series was measured to be $(8.1 \pm 1.5)\mu b$. This value has to be compared with the values $(11 \pm 3)\mu b$ and $(8 \pm 2)\mu b$, obtained in a multichannel analysis of the $K^- p \to \pi^+\pi^+\pi^-\Sigma^-$ final state in a fit of the 3π mass distribution. These results are in fairly good agreement. On the other hand, the experimental moment of the Dalitz series obtained using the very forward produced events ($\cos\theta_{p,\Sigma^-} > 0.7$) shows no signal in the A_2 region indicating that A_2 forward production is strongly suppressed. This is expected, since it would require the exchange of a double charged strange meson.

5. CONCLUSIONS

In this paper we have presented a symmetrical three-body formalism to obtain the DA of several 3π states. The DA is a set of moments of orthonormal functions of the DP variables, characterizing the DP decay distribution of a given resonance. The Dalitz series, constructed from the DA, provides a powerful tool to detect known resonances produced in complicated final states and to measure the corresponding cross sections. The method has been applied successfully to the resonances ω, ϕ and A_2 observed in the $K^-p \rightarrow \pi^+\pi^-\pi^0\Lambda$ reaction. A tentative determination of the DA for the backwardly produced A_1 in the process $K^-p \rightarrow \pi^+\pi^+\pi^-\Sigma^-$ is also given. We believe that an analysis in terms of the DA for the 3π system diffractively produced and for the one observed in τ decays will probably clarify our present knowledge on the A_1. The application of this formalism to other final states might prove to be rewarding.

Acknowledgements

We wish to thank the members of the ACNO Collaboration not only for making their data accessible to us but also for their encouragement and for many profitable discussions. Two of us, M. Aguilar-Benitez and M.G. Doncel thank also the CERN EP-Division for his hospitality.

REFERENCES

[1] B.C. Maglić, L.W. Alvarez, A.H. Rosenfeld and M.L. Stevenson, Phys. Rev. Lett. 7 (1961) 178.

[2] R. Armenteros, R. Budde, L. Montanet, D.R.O. Morrison, S. Nilsson, A. Shapira, J. Vandermeulen, C. d'Andlau, A. Astier, C. Ghesquière, B. Gregory, D. Rahm, P. Rivet and F. Solmitz, Proceedings of the 1962 International Conference on High Energy Physics at CERN (1962) 90.

[3] C. Zemach, Phys. Rev. 133B (1964) 1201.

[4] F.T. Smith, Phys. Rev. 120 (1960) 1058;

J. Math. Phys. 3 (1962) 735.

[5] A.J. Dragt, J. Math, Phys. 6 (1965) 533, 1621.

[6] B.W. Lee, New Phys., Korean Physical Society, 7 (1968) 41.

[7] F. del Aguila and M.G. Doncel, to be published;

F. del Aguila, Thesis, Universidad Autonoma de Barcelona (1979).

[8] M. Cerrada, F. Wagner, V. Chaloupka, R.J. Hemingway, S.O. Holmgren, M.J. Losty, R. Blokzijl, G.G.G. Massaro, G.F. Wolters, P.M. Heinen, E.W. Kittel, W.J. Metzger, J.S.M. Vergeest, B. Foster and J. Wells, Nucl. Phys. B126 (1977) 241.

[9] M.J. Losty, S.O. Holmgren, M. Aguilar-Benitez, F. Barreiro, R.J. Hemingway, R.P. Worden, G.G.G. Massaro, R. Blokzijl, J.C. Kluyver, G.F. Wolters, J.J. Timmermans, J.S.M. Vergeest, R.T. Van de Walle, J. Wells, B. Foster, P. Grossmann and L. Lyons, Nucl. Phys. B133 (1978) 38.

[10] Ph. Gavillet, P. Berge, A. Ferrando, R. Hemingway, S.O. Holmgren, M. Losty, J.C. Marin, L. Montanet, E. Pagiola, N. Yamdagni, R. Blokzijl, B. Jongejans, J.C. Kluyver, G.G.G. Massaro, J. Engeler, W. Kittel, J. Vergeest, R. Van de Walle, B. Foster, P. Grossman, P. Lamb and W.L. McDowell, Phys. Lett. 69B (1977) 119.

TABLE CAPTIONS

Table 1 Definitions of the DP variables ρ and ϕ and the DP functions $G^{\lambda\mu}(\rho, \phi)$ used in this paper (we assume that the three pions have equal mass m).

Table 2 First allowed amplitudes $a^{\lambda\mu(\delta_1)}$ and coefficients giving the moments $q^{\lambda\mu}$ as quadratical functions of these amplitudes, for the different cases treated in the text.

Table 3 DA's and decay amplitudes for ω, ϕ, A_2 and A_1 (by convention, the first amplitude is real and positive and the imaginary part of the second one is positive).

TABLE 1

(a) DP variables ρ and ϕ as functions of the triangular variables s_1, s_2, s_3 (effective mass squared of the three two-body subsystems) and of the invariant mass M of the three-body system. We use the polar coordinates of the DP r and θ and the value of the radius $r_B(\theta)$ corresponding to the boundary:

$$r\cos\theta = (-3s_3 + M^2 + 3m^2)/2M(M-3m),$$

$$r\sin\theta = \sqrt{3}(s_1 - s_2 - 3m^2)/2M(M-3m),$$

$$r_B(\theta) = (M + 3m)/2(M^2 + 3m^2)^{\frac{1}{2}} \cos(\chi/3),$$

$$\mathrm{tg}\chi = [(M^2+ 3m^2)^3/M^2(M^2 - 9m^2)^2 - \cos^2(3\theta)]^{\frac{1}{2}}/\cos(3\theta),$$

$$0 \leq \chi < \pi,$$

$$\rho = r/r_B(\theta),$$

$$\phi = 2\pi\int_0^\theta r_B(\theta')\,d\theta'/\int_0^{2\pi} r_B(\theta')\,d\theta'$$

(b) DP functions $G^{\lambda\mu}(\rho, \phi)$

$$G^{0,0} = 1,$$

$$G^{4,0} = \sqrt{3}(1-2\rho^2),$$

$$G^{8,0} = \sqrt{5}(1-6\rho^2+6\rho^4),$$

$$G^{12,0} = \sqrt{7}(1-12\rho^2+30\rho^4-20\rho^6),$$

$$G^{16,0} = \sqrt{9}(1-20\rho^2+90\rho^4-140\rho^6+70\rho^8),$$

$$G^{2,2} = \sqrt{2}\, e^{i\phi},$$

$$G^{6,2} = \sqrt{4}\, e^{i\phi}\rho(2-3\rho^2),$$

$$G^{10,2} = \sqrt{6}\, e^{i\phi}\rho(3-12\rho^2+10\rho^4),$$

$$G^{4,4} = \sqrt{3}\, e^{2i\phi}\rho^2,$$

$$G^{8,4} = \sqrt{5}\, e^{2i\phi}\rho^2(3-4\rho^2),$$

$$G^{6,6} = \sqrt{4}\, e^{3i\phi}\rho^3,$$

$$G^{10,6} = \sqrt{6}\, e^{3i\phi}\rho^3(4-5\rho^2),$$

$$G^{14,6} = \sqrt{8}\, e^{3i\phi}\rho^3(10-30\rho^2+21\rho^4),$$

$$G^{12,12} = \sqrt{7}\, e^{6i\phi}\rho^6,$$

$$G^{16,12} = \sqrt{9}\, e^{6i\phi}\rho^6(7-8\rho^2).$$

TABLE 2

(a)

$\omega, \phi(I, J^P = 0,1^-) \rightarrow \pi^+\pi^-\pi^0$ a^{20}; a^{60}; $a^{86} = a^{8-6}$

	$\lvert a^{20}\rvert^2$	$\lvert a^{60}\rvert^2$	$\lvert a^{86}\rvert^2$	Re $\overline{a^{20}a^{60}}$	Re $\overline{a^{20}a^{86}}$	Re $\overline{a^{60}a^{86}}$
$q^{0,0}$	1	1	2	0	0	0
$q^{4,0}$	$\sqrt{1/3}$	$\sqrt{1/75}$	$-\sqrt{4/3}$	$\sqrt{8/3}$	0	0
$q^{8,0}$	0	$\sqrt{1/5}$	$-\sqrt{20/49}$	$\sqrt{8/5}$	0	0
$q^{12,0}$	0	$\sqrt{81/175}$	$\sqrt{4/7}$	0	0	0
$q^{16,0}$	0	0	$-4/21$	0	0	0
$q_R^{6,6}$	0	0	0	0	$\sqrt{16/5}$	$-\sqrt{32/5}$
$q_R^{10,6}$	0	0	0	0	$\sqrt{32/15}$	$-\sqrt{256/735}$
$q_R^{14,6}$	0	0	0	0	0	$\sqrt{80/49}$
$q_R^{12,12}$	0	0	$\sqrt{25/14}$	0	0	0
$q_R^{16,12}$	0	0	$\sqrt{25/18}$	0	0	0

TABLE 2 (Cont'd)

(b) $A_2(I,\ J^P = 1,2^+) \to \pi^+\pi^-\pi^0$

$a^{31(0-1)} = -a^{3-1(01)}$; $a^{51(0,1)} = -a^{5-1(01)}$; $a^{53} = -a^{5-3}$; $a^{71(0-1)} = -a^{7-1(01)}$

	$\lvert a^{31}\rvert^2$	$\lvert a^{51}\rvert^2$	$\lvert a^{53}\rvert^2$	$\lvert a^{71}\rvert^2$	Re $\overline{a^{31}}a^{51}$	Re $\overline{a^{31}}a^{53}$	Re $\overline{a^{31}}a^{71}$	Re $\overline{a^{51}}a^{53}$	Re $\overline{a^{51}}a^{71}$	Re $\overline{a^{53}}a^{71}$
$q^{0,0}$	2	2	4/5	2	0	0	0	0	0	0
$q^{4,0}$	$\sqrt{4/3}$	$\sqrt{1/3}$	0	$\sqrt{3/25}$	$\sqrt{8/3}$	0	$\sqrt{8}$	0	-2/5	0
$q^{8,0}$	0	$-\sqrt{1/5}$	$-\sqrt{16/125}$	$\sqrt{1/5}$	$\sqrt{8/5}$	0	$\sqrt{24/5}$	0	$\sqrt{12/5}$	0
$q^{12,0}$	0	0	0	$\sqrt{144/175}$	0	0	0	0	$\sqrt{432/175}$	0
$q_R^{2,2}$	-2/3	1/6	0	-3/10	$\sqrt{32/9}$	$\sqrt{32/15}$	0	$-\sqrt{4/15}$	$-\sqrt{3}$	$-\sqrt{4/5}$
$q_R^{6,2}$	$-\sqrt{2/9}$	$\sqrt{128/225}$	0	0	4/3	$\sqrt{16/15}$	$-\sqrt{48/25}$	$\sqrt{32/375}$	0	$\sqrt{32/125}$
$q_R^{10,2}$	0	$\sqrt{27/100}$	0	$-\sqrt{75/196}$	0	0	$-\sqrt{32/25}$	$\sqrt{36/125}$	1	$\sqrt{108/125}$
$q_R^{14,2}$	0	0	0	-24/35	0	0	0	0	0	0
$q_R^{4,4}$	0	0	0	0	0	$-\sqrt{4/5}$	0	$\sqrt{8/5}$	0	$\sqrt{24/125}$
$q_R^{8,4}$	0	0	0	0	0	$-\sqrt{12/25}$	0	$\sqrt{24/25}$	0	$-\sqrt{16/50}$
$q_R^{12,4}$	0	0	0	0	0	0	0	0	0	$-\sqrt{512/875}$
$q_R^{6,6}$	0	0	$-\sqrt{72/625}$	0	0	0	0	0	0	0
$q_R^{10,6}$	0	0	$-\sqrt{48/625}$	0	0	0	0	0	0	0

TABLE 2 (Cont'd)

(c)

$A_1(I,\ J^P = 1,1^+) \to \pi^+\pi^+\pi^-$

$a^{11(0-1)} = a^{1-1(01)}$; $a^{31(0-1)} = a^{3-1(01)}$; $a^{33} = a^{3-3}$

	$\lvert a^{11}\rvert^2$	$\lvert a^{31}\rvert^2$	$\lvert a^{33}\rvert^2$	Re $\overline{a^{11}}a^{31}$	Re $\overline{a^{11}}a^{33}$	Re $\overline{a^{31}}a^{33}$
$q^{0,0}$	2	2	16/5	0	0	0
$q^{4,0}$	0	0	$-\sqrt{256/75}$	$\sqrt{16/3}$	0	0
$q_R^{2,2}$	1	-1/3	0	-2	$-\sqrt{64/5}$	$\sqrt{64/45}$
$q_R^{6,2}$	0	$-\sqrt{8/9}$	0	0	0	$-\sqrt{128/45}$
$q_R^{4,4}$	0	0	0	0	$-\sqrt{128/15}$	$\sqrt{128/15}$
$q_R^{6,6}$	0	0	$\sqrt{128/25}$	0	0	0

(d)

$A_1(I,\ J^P = 1,1^+) \to \pi^+\pi^-\pi^0$

$a^{11(0-1)} = a^{1-1(01)}$; $a^{31(0-1)} = a^{3-1(01)}$; $a^{33} = a^{3-3}$

	$\lvert a^{11}\rvert^2$	$\lvert a^{31}\rvert^2$	$\lvert a^{33}\rvert^2$	Re $\overline{a^{11}}a^{31}$	Re $\overline{a^{11}}a^{33}$	Re $\overline{a^{31}}a^{33}$
$q^{0,0}$	2	2	4/5	0	0	0
$q^{4,0}$	0	0	$-\sqrt{16/75}$	$\sqrt{16/3}$	0	0
$q_R^{2,2}$	1	-1/3	0	-2	$\sqrt{16/5}$	$-\sqrt{16/45}$
$q_R^{6,2}$	0	$-\sqrt{8/9}$	0	0	0	$\sqrt{32/45}$
$q_R^{4,4}$	0	0	0	0	$\sqrt{32/15}$	$-\sqrt{32/15}$
$q_R^{6,6}$	0	0	$\sqrt{8/25}$	0	0	0

TABLE 3

(a) $\omega \to \pi^+\pi^-\pi^0$	(b) $\phi \to \pi^+\pi^-\pi^0$	(c) $A_2^0 \to \pi^+\pi^-\pi^0$, $A_2^+ \to \pi^+\pi^+\pi^-$	(d) $A_1^+ \to \pi^+\pi^+\pi^-$	(e) $A_1^0 \to \pi^+\pi^-\pi^0$
$q^{0,0} = 1.000 \pm 0.015$	$q^{0,0} = 1.000 \pm 0.085$	$q^{0,0} = 1.000 \pm 0.072$	$q^{0,0} = 1.000 \pm 0.167$	$q^{0,0} = 1.000 \pm 0.210$
$q^{4,0} = 0.542 \pm 0.014$	$q^{4,0} = 0.353 \pm 0.054$	$q^{4,0} = 0.950 \pm 0.082$	$q^{4,0} = 0.255 \pm 0.146$	$q^{4,0} = 0.381 \pm 0.172$
$q^{8,0} = 0.005 \pm 0.013$	$q^{8,0} = -0.107 \pm 0.040$	$q^{8,0} = 0.782 \pm 0.069$	$q_R^{2,2} = 0.376 \pm 0.117$	$q_R^{2,2} = -0.218 \pm 0.358$
$q^{12,0} = 0.027 \pm 0.012$	$q^{12,0} = 0.047 \pm 0.015$	$q^{12,0} = 0.417 \pm 0.055$	$q_R^{6,2} = 0.037 \pm 0.036$	$q_R^{6,2} = -0.148 \pm 0.113$
$q^{16,0} = 0.000 \pm 0.000$	$q^{16,0} = -0.009 \pm 0.004$	$q_R^{2,2} = -0.259 \pm 0.036$	$q_R^{4,4} = 0.180 \pm 0.098$	$q_R^{4,4} = -0.104 \pm 0.056$
$q_R^{6,6} = 0.022 \pm 0.007$	$q_R^{6,6} = 0.174 \pm 0.036$	$q_R^{6,2} = -0.247 \pm 0.043$	$q_R^{6,6} = 0.125 \pm 0.095$	$q_R^{6,6} = 0.036 \pm 0.028$
$q_R^{10,6} = 0.019 \pm 0.007$	$q_R^{10,6} = 0.100 \pm 0.021$	$q_R^{10,2} = -0.274 \pm 0.050$		
$q_R^{14,6} = 0.001 \pm 0.006$	$q_R^{14,6} = -0.036 \pm 0.018$	$q_R^{14,2} = -0.193 \pm 0.031$		
$q_R^{12,12} = 0.000 \pm 0.001$	$q_R^{12,12} = 0.060 \pm 0.026$			
$q_R^{16,12} = 0.000 \pm 0.000$	$q_R^{16,12} = 0.053 \pm 0.023$			
$a^{20} = 0.98 \pm 0.01$	$a^{20} = 0.94 \pm 0.04$	$a^{31} = 0.42 \pm 0.07$	$a^{11} = 0.58 \pm 0.11$	As in (d) above, up to an overall factor.
$\mathrm{Re}\, a^{60} = -0.01 \pm 0.01$	$\mathrm{Re}\, a^{60} = -0.07 \pm 0.04$	$\mathrm{Re}\, a^{51} = 0.14 \pm 0.06$	$\mathrm{Re}\, a^{31} = 0.27 \pm 0.14$	
$\mathrm{Im}\, a^{60} = 0.20 \pm 0.04$	$\mathrm{Im}\, a^{60} = 0.12 \pm 0.07$	$\mathrm{Im}\, a^{51} = 0.16 \pm 0.15$	$\mathrm{Im}\, a^{31} = 0.08 \pm 0.28$	
$\mathrm{Re}\, a^{86} = 0.01 \pm 0.01$	$\mathrm{Re}\, a^{86} = 0.06 \pm 0.02$	$\mathrm{Re}\, a^{71} = 0.48 \pm 0.11$	$\mathrm{Re}\, a^{33} = -0.22 \pm 0.14$	
$\mathrm{Im}\, a^{86} = 0.00 \pm 0.03$	$\mathrm{Im}\, a^{86} = -0.20 \pm 0.05$	$\mathrm{Im}\, a^{71} = 0.22 \pm 0.21$	$\mathrm{Im}\, a^{33} = -0.08 \pm 0.24$	

FIGURE CAPTIONS

Fig. 1 Mass distribution of the $(\pi^+\pi^-\pi^0)$ system in the reaction $K^-p \rightarrow (\pi^+\pi^-\pi^0)\Lambda$. The shaded events have $\cos\theta_{p,\Lambda} > 0.7$.

Fig. 2 Experimental moments $Q^{\lambda\mu}$ as functions of $\pi^+\pi^-\pi^0$ mass in the ω region $0.73 < M(3\pi) < 0.83$ GeV. The solid lines are the results of the fit (see text) and the dashed ones describe the background contribution $B^{\lambda\mu}$. The DA can be estimated by the height of the different Breit Wigner's.

Fig. 3 Experimental moments $Q^{\lambda\mu}$ as functions of $\pi^+\pi^-\pi^0$ mass in the ϕ region $1.005 < M(3\pi) < 1.045$ GeV. The extra cut $0.65 < \cos\theta_{p,\Lambda} < 1.0$ has been imposed.

Fig. 4 Experimental moments $Q^{\lambda\mu}$ as functions of $\pi^+\pi^-\pi^0$ mass in the A_2 region $1.1 < M(3\pi) < 1.5$ GeV. Events with $1.34 < M(\Lambda\pi^{+0}) < 1.44$ GeV and $\cos\theta_{p,\Lambda} < 0.75$ have been removed.

Fig. 5 (a) Mass distribution of the 3π system for events with $\cos\theta_{p,\Lambda} > 0$.

(b) Experimental moments of the A_2 Dalitz series as a function of 3π mass for events in fig. 5(a). The solid line is the result of a fit to an A_2 Breit-Wigner shape (mass and width fixed) plus a smooth polynomial background (dashed line in the plot).

(c) and (d) Same as figs 5(a) and (b) for events with $\cos\theta_{p,\Lambda} < 0$.

Fig. 6 Mass distribution of the $(\pi^+\pi^+\pi^-)$ system in the reaction $K^-p \rightarrow (\pi^+\pi^+\pi^-)\Sigma^-$ for events with $\cos\theta_{p,\Sigma^-} < -0.75$. The shaded events have at least a $(\pi^+\pi^-)$ combination with $0.62 < M(\pi^+\pi^-) < 0.88$ GeV.

Fig. 7 Experimental moments $Q^{\lambda\mu}$ as functions of the $\pi^+\pi^+\pi^-$ mass in the region $0.41 < M(3\pi) < 1.45$ GeV. The solid lines are the results of the fit described in the text. The dashed lines describe the background under the A_2 and A_1 resonances.

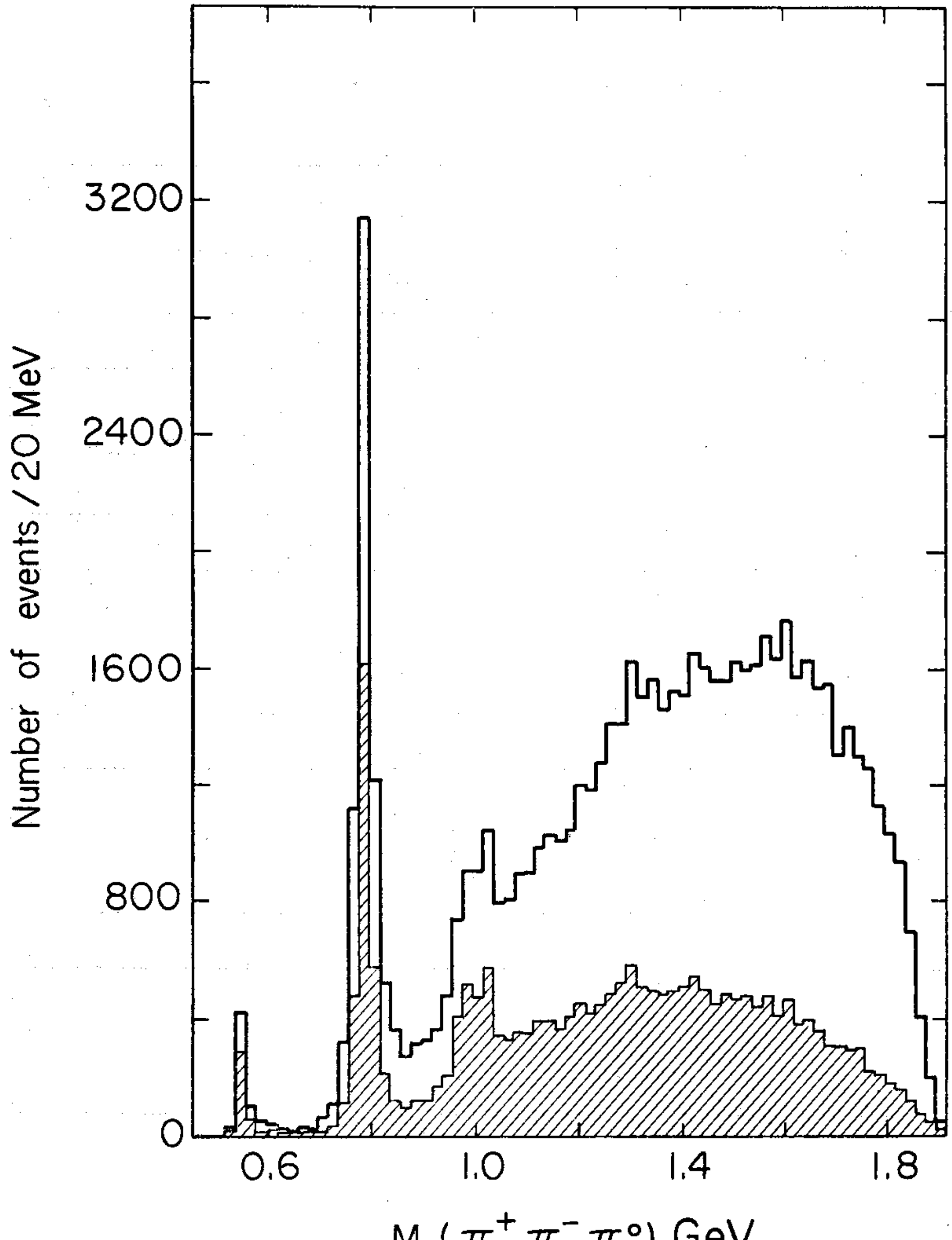

Number of events / 20 MeV
3200
2400
1600
800
0
0.6
1.0
1.4
1.8
M ($\pi^+ \pi^- \pi^\circ$) GeV

fig. 1

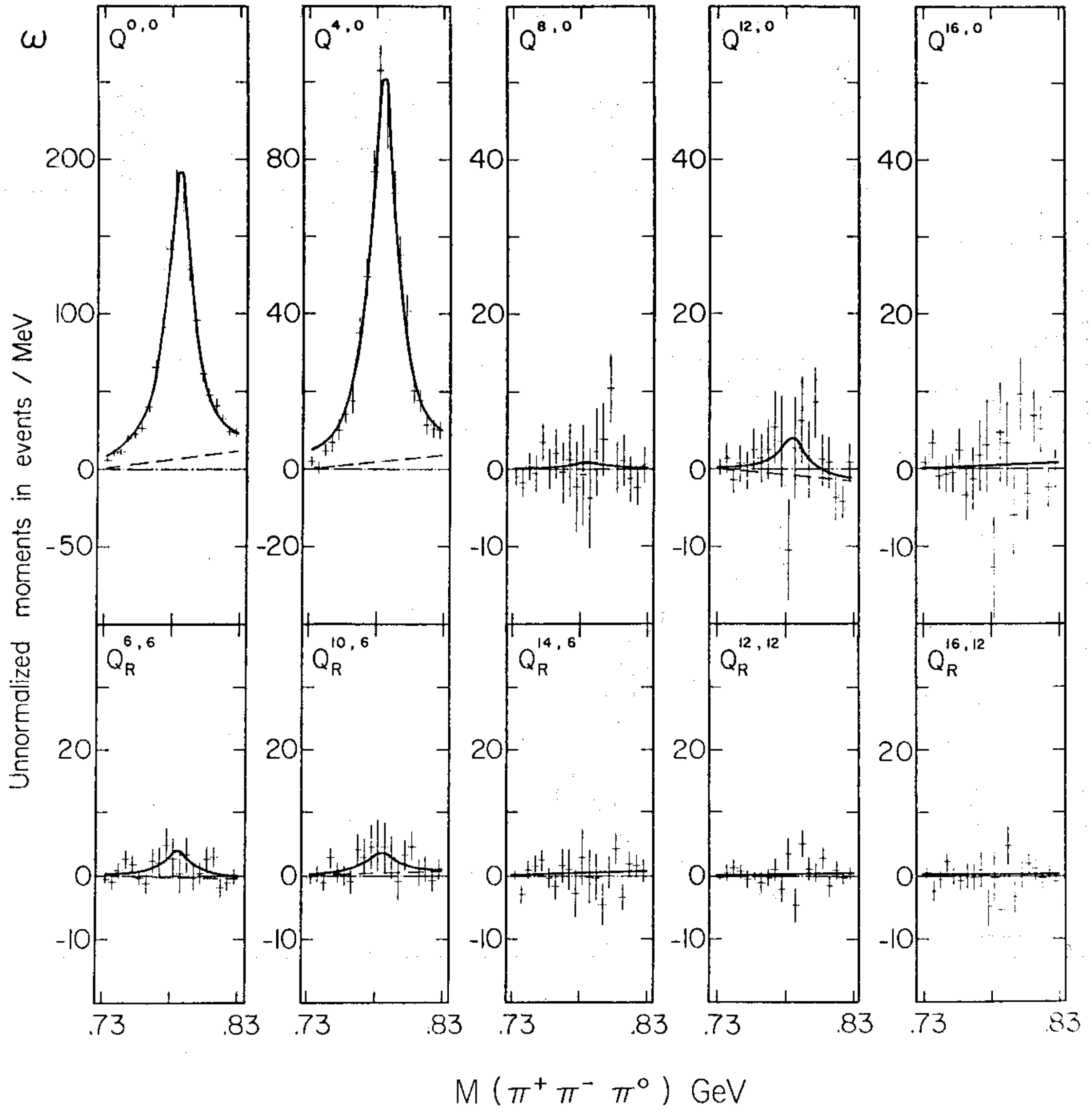
ω
$Q^{0,0}$
$Q^{4,0}$
$Q^{8,0}$
$Q^{12,0}$
$Q^{16,0}$
$Q_R^{6,6}$
$Q_R^{10,6}$
$Q_R^{14,6}$
$Q_R^{12,12}$
$Q_R^{16,12}$
Unnormalized moments in events / MeV
$M(\pi^+ \pi^- \pi^o)$ GeV

fig. 2

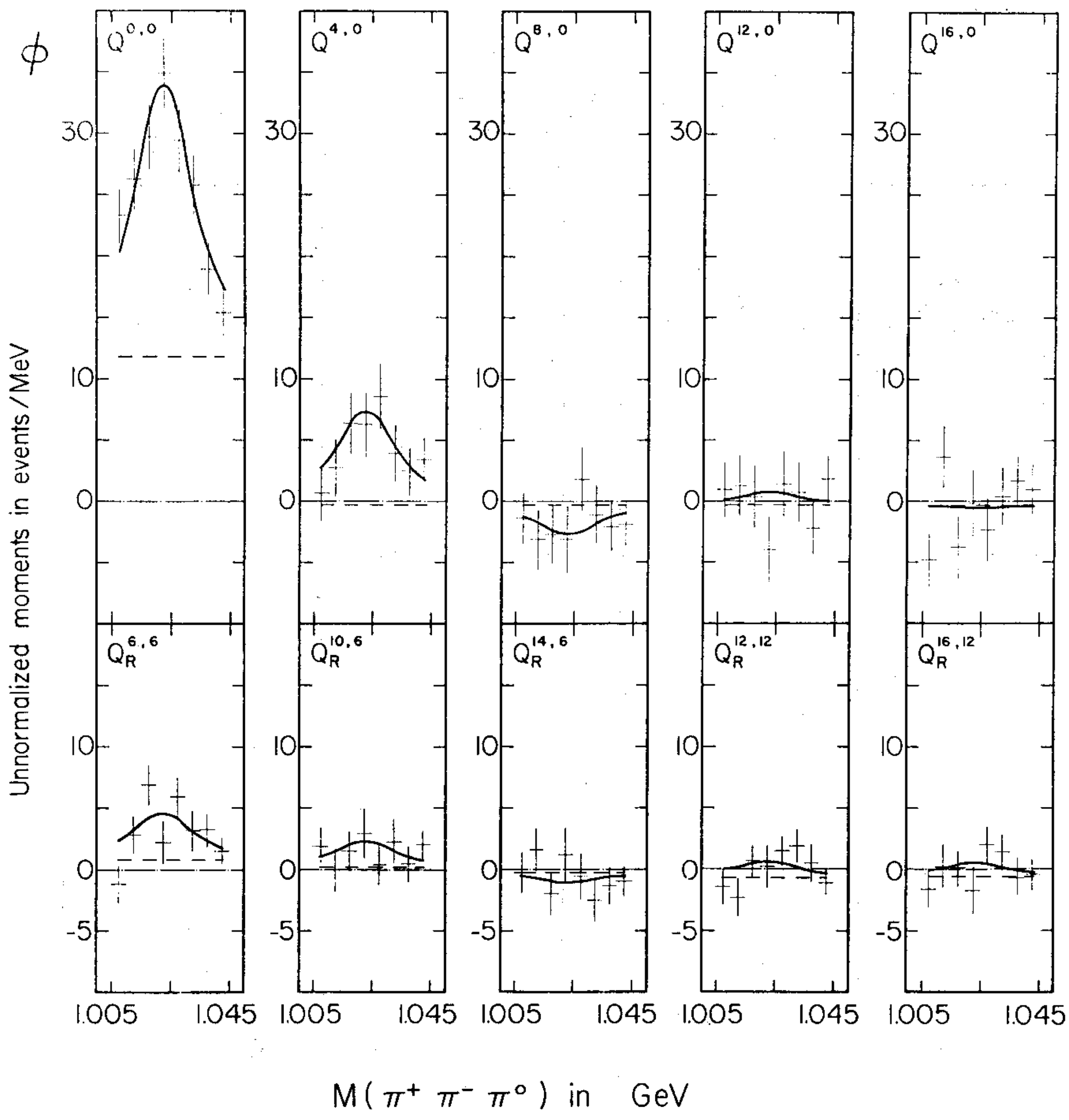

φ
Unnormalized moments in events/MeV
$Q^{0,0}$
$Q^{4,0}$
$Q^{8,0}$
$Q^{12,0}$
$Q^{16,0}$
$Q_R^{6,6}$
$Q_R^{10,6}$
$Q_R^{14,6}$
$Q_R^{12,12}$
$Q_R^{16,12}$
30
10
0
-5
1.005
1.045
M($\pi^+ \pi^- \pi^\circ$) in GeV

fig. 3

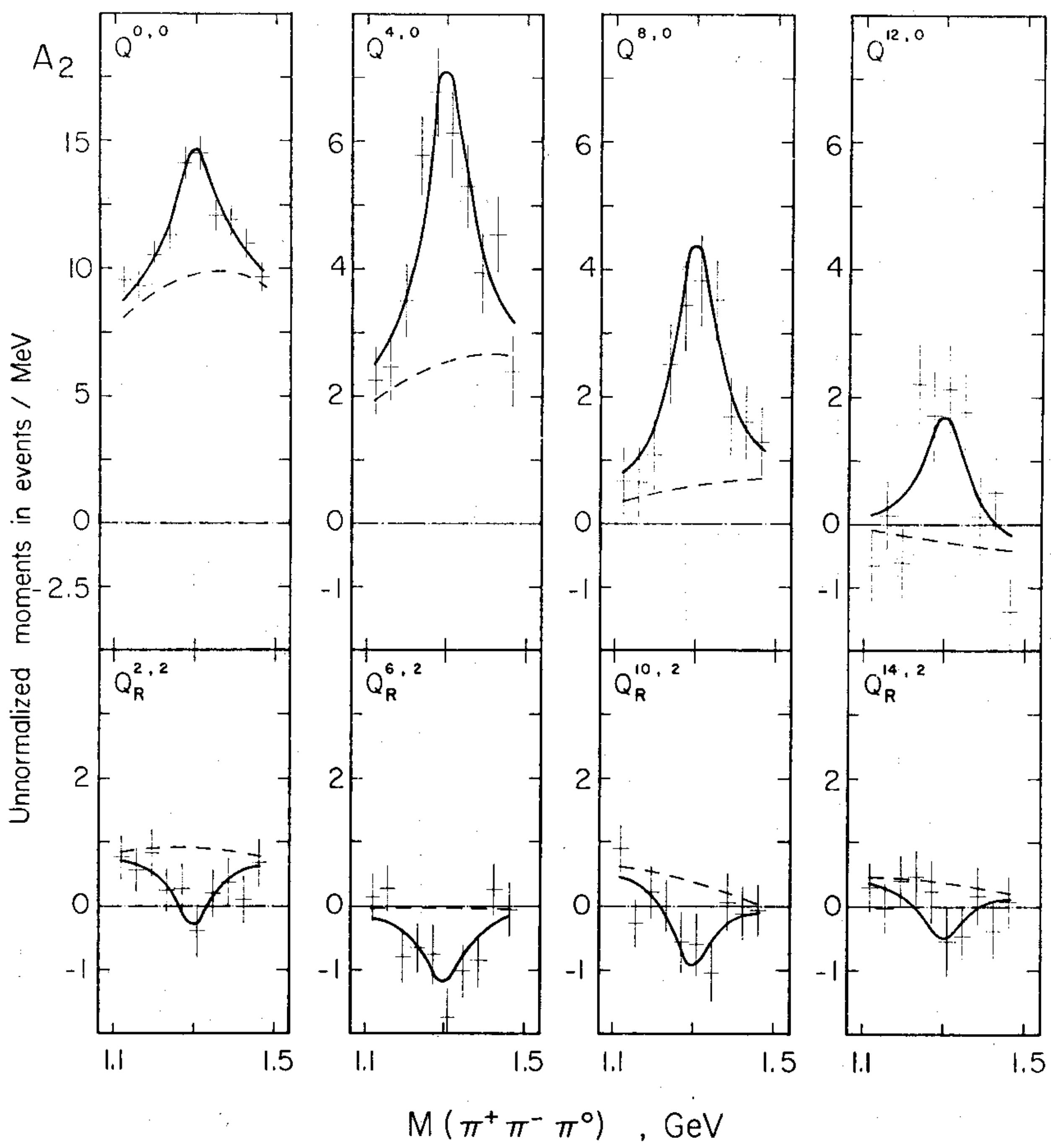
A2
Q0,0
Q4,0
Q8,0
Q12,0
Q_R2,2
Q_R6,2
Q_R10,2
Q_R14,2
Unnormalized moments in events / MeV
15
10
5
0
-2.5
6
4
2
-1
1.1
1.5
M (π+ π- π°) , GeV

fig 4

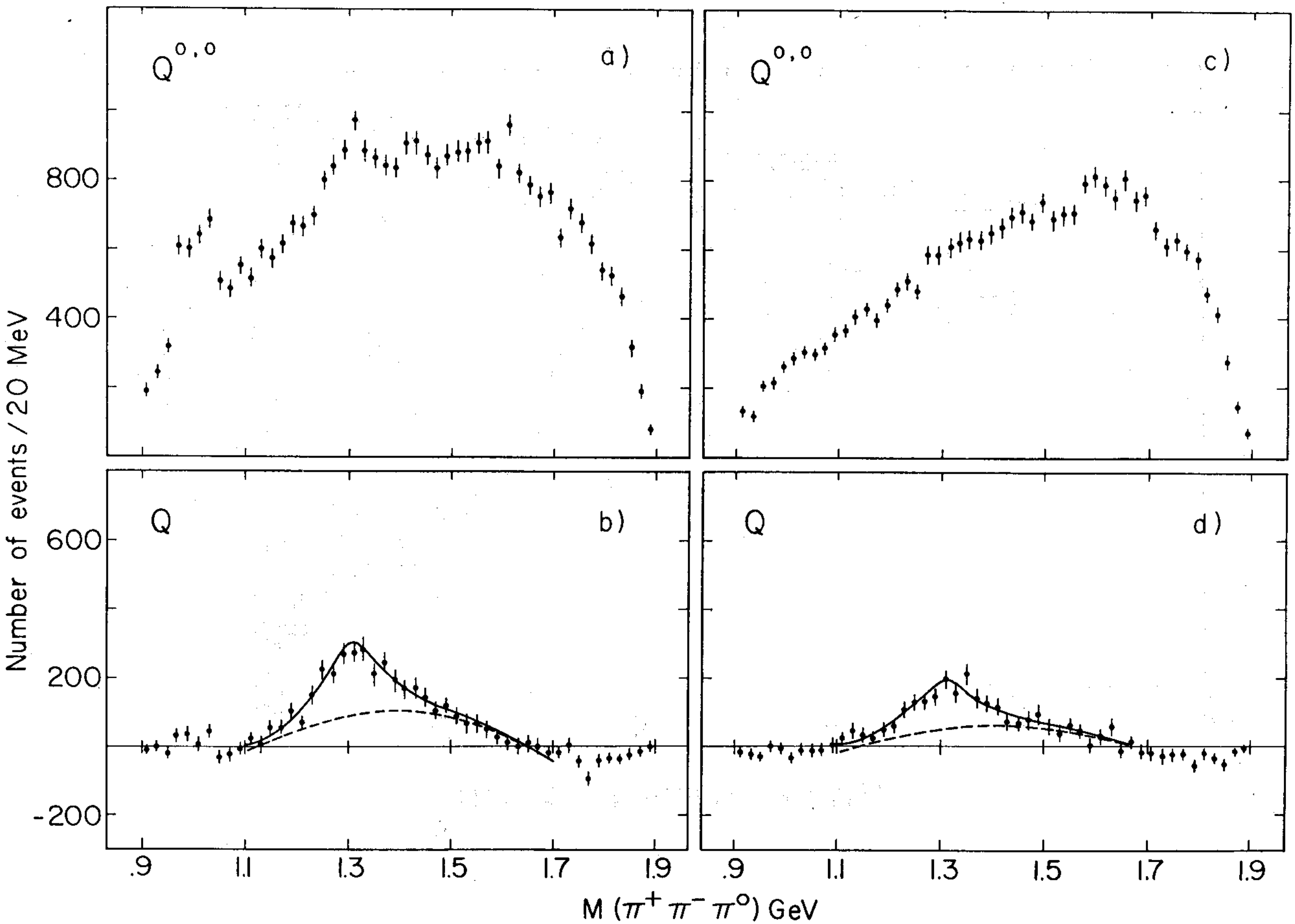

$Q^{o,o}$
a)
$Q^{o,o}$
c)
Q
b)
Q
d)
800
400
600
200
-200
Number of events / 20 MeV
.9
1.1
1.3
1.5
1.7
1.9
$M(\pi^+ \pi^- \pi^o)$ GeV

fig. 5

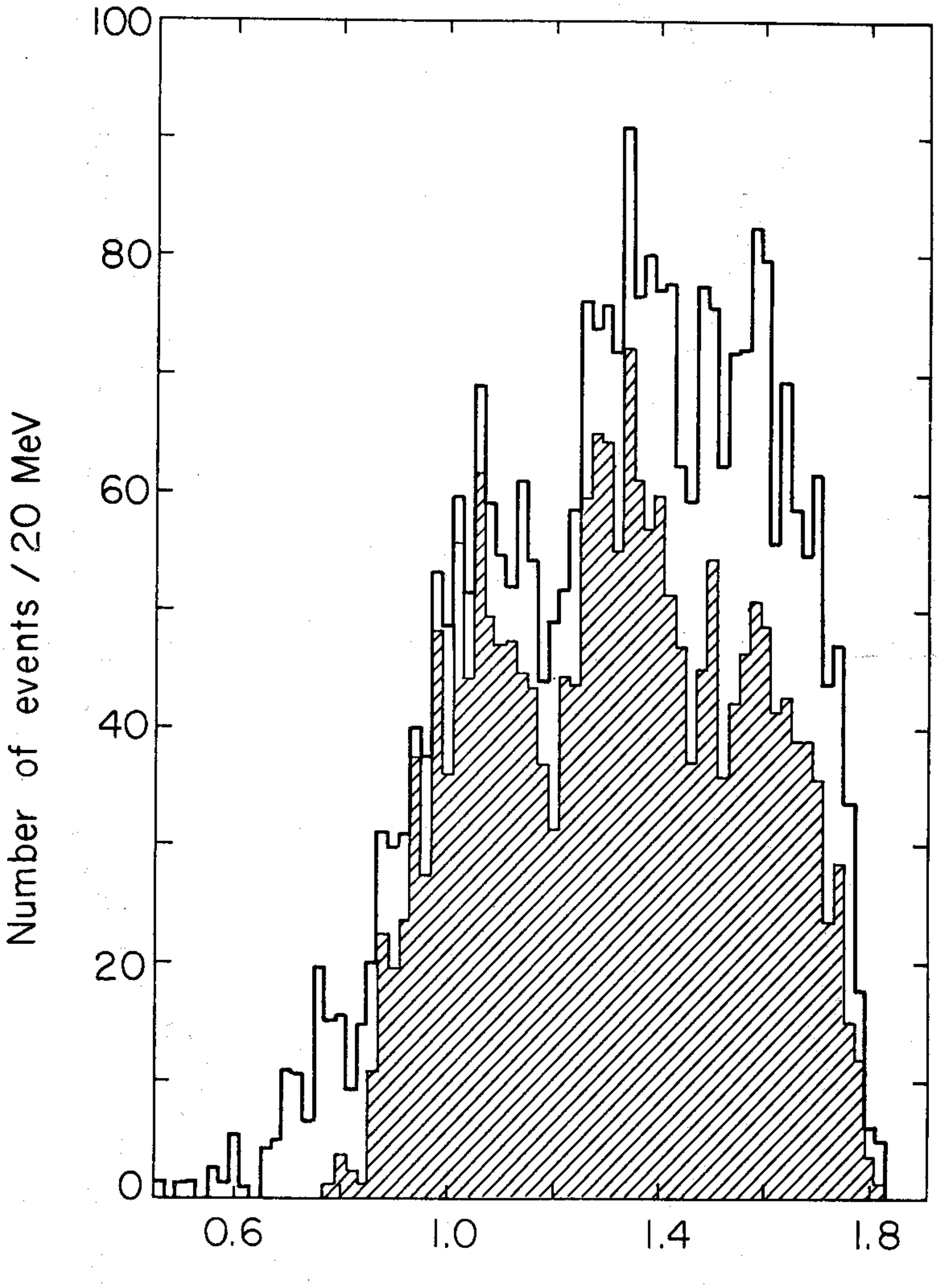

fig. 6

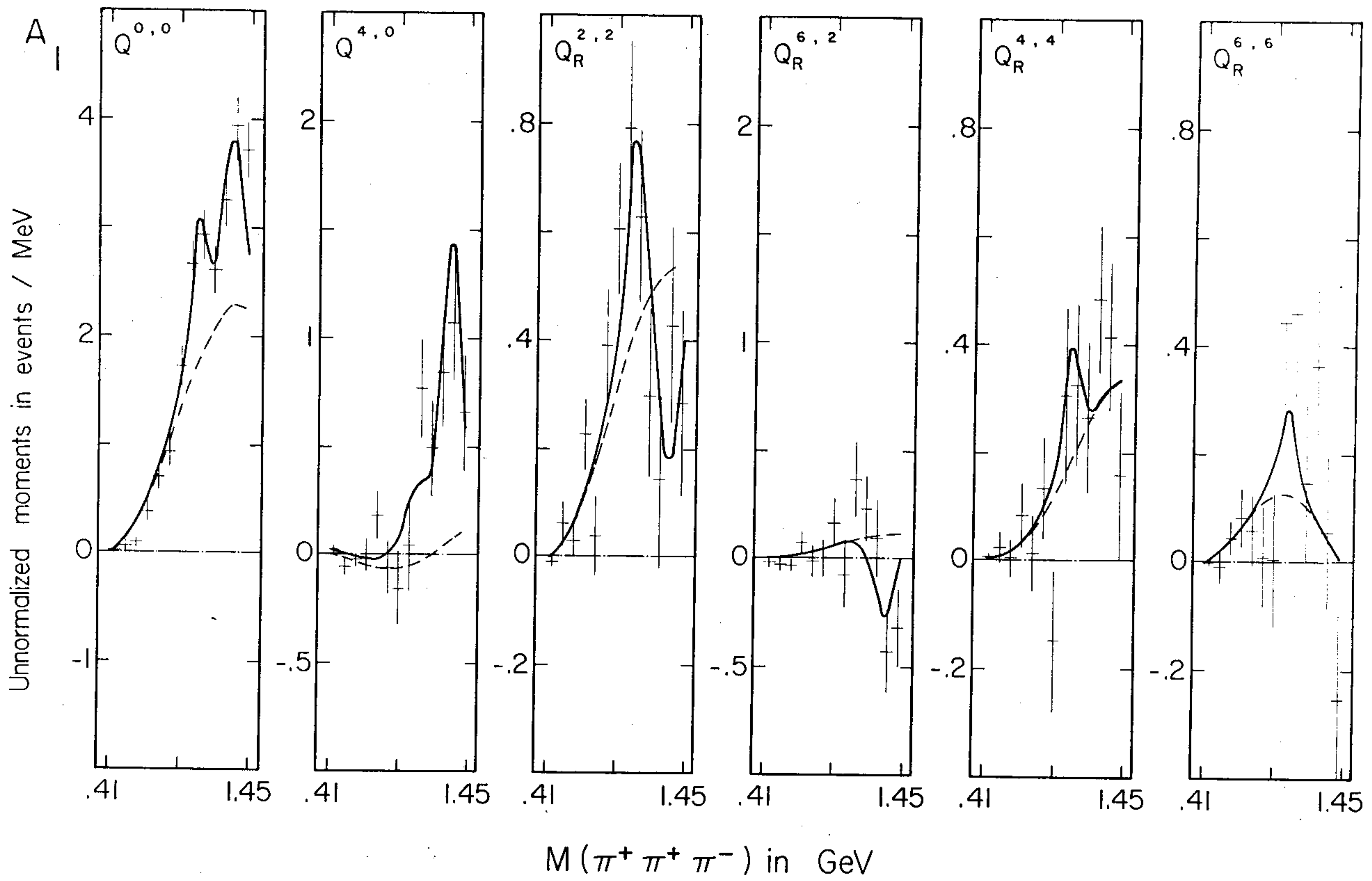

A1
Q^0,0
Q^4,0
Q_R^2,2
Q_R^6,2
Q_R^4,4
Q_R^6,6
4
2
0
-1
2
1
0
-.5
.8
.4
0
-.2
2
1
0
-.5
.8
.4
0
-.2
.8
.4
0
-.2
.41
1.45
Unnormalized moments in events / MeV
M(π+ π+ π−) in GeV

fig.7